RSC Advances

PAPER

View Article Online
View Journal | View Issue

Open Access Article. Published on 19 January 2026. Downloaded on 3/14/2026 7:06:49 AM.
This article is licensed under a Creative Commons Attribution-NonCommercial 3.0 Unported Licence.

Check for updates

Cite this: *RSC Adv.*, 2026, **16**, 4045

Thermo-responsive polysulfobetaine beads crosslinked with biodegradable alginates for controlled release of agricultural pesticide

Brandon Andrade-Gagnon,[a] Chloe Olszewski,[a] Kamaljeet Kaur Bawa,[a] Usha D. Hemraz*[b] and Jung Kwon Oh *[a]

Received 10th November 2025
Accepted 11th January 2026

DOI: 10.1039/d5ra08674d

rsc.li/rsc-advances

The rise in global food demand and the loss in crop production by pests highlight the need for efficient pesticide delivery systems. Stimuli-responsive degradation with thermoresponsive polymers is a promising platform that offers the controlled release of pesticides. Here, we report the development of millimeter-sized thermoresponsive beads (m-beads) composed of a zwitterionic polysulfobetaine exhibiting upper critical solution temperature (UCST) behavior, crosslinked with biodegradable alginate *via* supramolecular ionic interactions with calcium ions in water. The fabricated m-beads are capable of encapsulating fluorescein and glufosinate ammonium pesticide with encapsulation efficiency greater than 99%. Promisingly, they exhibit enhanced release with an increasing amount of alginate in m-beads as well as at a temperature above the UCST. This work highlights the potential of UCST-type polysulfobetaine-based m-beads as a smart delivery platform, offering environmentally-triggered release of pesticides.

Introduction

Global population growth continues to intensify the demand for enhanced agricultural productivity. This challenge is further compounded by climate change, shifting consumption patterns, the reduction of arable land, and persistent pest infestations, all of which contribute to substantial yield losses in major crops.[1–3] Pesticides remain essential tools for safeguarding crop yields; however, conventional application methods, such as foliar spraying, suffer from significant inefficiencies. Losses through degradation, photolysis, evaporation, and surface runoff not only reduce field efficacy but also contribute to environmental contamination, non-target toxicity, and the emergence of pest resistance.[4–6] Although organic agriculture offers environmental benefits, complete dependence on such practices would likely lead to reduced productivity and increased food insecurity. Consequently, improving the efficiency and sustainability of pesticide use remains a critical goal.[7] Wijerathna *et al.* demonstrated that thiamethoxam seed treatment provided extended protection of faba bean yields against the pea leaf weevil compared with foliar application of lambda-cyhalothrin,[8–10] highlighting the importance of pesticide residual life in effective pest management strategies, with a longer residual life being more lethal to pest over an extended period.[8–13]

Controlled-release pesticide systems offer a viable strategy to overcome the limitations of conventional formulations by enabling sustained, targeted delivery with greater precision, increasing the residual half-life of the pesticide to tackle the pest, thereby reducing overall chemical usage. In addition to promoting sustainability, such systems can improve efficacy, minimize ecological impact, lower application frequency and labor costs.[7–10] Among the various strategies developed to enhance the efficiency and sustainability of pesticide application, the encapsulation of pesticides within polymeric microparticles has emerged as a particularly favorable option. Most existing microparticle formulations depend primarily on passive diffusion mechanisms to release their contents, preventing the system from adapting to changing environmental conditions—such as fluctuations in temperature, humidity, or the presence of pests.[11–16] As a result, there is a shortage in pesticide delivery and timing required to maximize efficacy and minimize environmental impact. To overcome the limitation of primary passive diffusion mechanism, the development of stimuli-responsive degradable nano-sized or micro-sized polymeric formulation has been explored as an alternative approach.[17–28]

Thermoresponsive materials offer a promising solution to address these limitations. Smart polymers can undergo physical or chemical changes in response to seasonal temperature changes, such as the onset of warmer spring or summer conditions, as well as daily temperature changes such as the onset of daytime conditions when pest populations typically

[a]*Department of Chemistry and Biochemistry, Concordia University, Montreal, Quebec, H4B 1R6, Canada. E-mail: john.oh@concordia.ca*

[b]*Human Health Therapeutics, National Research Council of Canada, 6100 Royalmount Avenue, Montreal, Quebec, H4P 2R2, Canada. E-mail: usha.hemraz@nrc-cnrc.gc.ca*

© 2026 The Author(s). Published by the Royal Society of Chemistry

Open Access Article. Published on 19 January 2026. Downloaded on 3/14/2026 7:06:49 AM.
This article is licensed under a Creative Commons Attribution-NonCommercial 3.0 Unported Licence.

increase. Such temperature changes could allow them to release their encapsulated pesticides selectively when environmental temperatures reach predefined thresholds.[29–31] The design of thermoresponsive polymers exhibit lower critical solution temperature (LCST) that undergo the change in their solution properties upon heating have been explored for the development of thermoresponsive controlled pesticide formulations.[32,33] In contrast, thermoresponsive polymers with upper critical solution temperature (UCST) undergo their phase transition from aggregate state to unimers being soluble in aqueous solution upon heating. Most promising UCST polymers include zwitterionic polymers, which are charge-neutral with both anionic and cationic groups along polymer backbone or side chains of typically phosphorylcholine, carboxybetaine, and sulfobetaine.[34–37] Despite these features of UCST thermoresponsive polymers, to our best knowledge, only few reports have described the fabrication of microbeads based on UCST polymers for encapsulation and controlled release of agrichemicals. For example, Qiu *et al.* reported the UCST behavior of enzymatic hydrolysis of lignin in water/ethanol mixture. The fabricated avermectin-loaded microspheres with an average diameter of 800 nm exhibit the enhanced release of avermectin at 50 °C (90%), compared with 25 °C (20%) over 24 h.[38]

In this work, we developed thermoresponsive millimeter-sized beads (m-beads) based on UCST polysulfobetaine crosslinked with biodegradable alginate (ALG) and investigated their capacity for pesticide encapsulation and controlled release in response to temperature variation. Poly(3-((2-(methacryloyloxy)-ethyl) dimethylammonio)propane-1-sulfonate) (**PDMAPS**), exhibiting UCST transition at 12 °C, was synthesized by free radical polymerization (FRP). We investigated the fabrication of thermoresponsive beads of UCST **PDMAPS**, aided with various amounts of biodegradable ALG, by physical crosslinking through supramolecular ionic interactions with calcium ions, as well as their encapsulation of fluorescein, a model pesticide and glufosinate ammonium (GFA), a commonly used pesticide. The beads composed of **PDMAPS** and ALG exhibit the enhanced release of encapsulated chemicals with an increasing amount of ALG, and promisingly at temperatures above the UCST of **PDMAPS**. These findings highlight the potential of UCST-based polymer-alginate systems as environmentally adaptive carriers for temperature-responsive pesticide delivery in sustainable agriculture.

Experimental

Materials

3-((2-(Methacryloyloxy)-ethyl)dimethylammonio)propane-1-sulfonate (**DMAPS**, 95%), ammonium persulfate (APS, 98%), sodium alginate (ALG), calcium chloride dihydrate ($CaCl_2 \cdot 2H_2O$, 99%), fluorescein, and glufosinate ammonium (GFA) were purchased from Sigma-Aldrich and used without further purification.

Instrumentation

^{1}H NMR spectra were recorded using a 300 MHz Bruker spectrometer and a 500 MHz Varian spectrometer. The D_2O singlet at 4.79 ppm was selected as the reference standard. UV/vis spectroscopy was conducted with an Agilent Cary 3500 double beam multicell UV/vis spectrophotometer using a 3 cm wide quartz cuvette. Differential scanning calorimetry (DSC) analysis was carried out to determine thermal properties including glass transition temperature (T_g) of crosslinked films with a TA Instruments DSC Q20 Differential Scanning Calorimeter. Samples were dried for 24 h in vacuum oven to remove residual solvents. Temperature ranged from −80 to 200 °C with heating and cooling cycles conducted at a rate of 10 °C min^{-1} (cycles: cool to −80 °C, heat up to 200 °C (1st run), cool to −80 °C, heat up to 200 °C (2nd run), and cool to 25 °C). T_g values were determined from the 2nd heating run. Thermogravimetric analysis (TGA) was conducted with a TA Instruments Q50 Analyzer. Dried samples (5–10 mg) were placed in a platinum pan inside a programmable furnace and then heated from 25 to 800 °C at a heating rate of 20 °C min^{-1} under nitrogen flow. Mass loss was then calculated. The hydrodynamic diameter of aqueous **PDMAPS** aggregates was measured by dynamic light scattering (DLS) at a fixed scattering angle of 173° at 25 °C with a Malvern Instruments Nano S ZEN1600 equipped with a 633 nm He–Ne gas laser. A Keyence digital microscope was used to measure the size and morphology of the m-beads, where the average diameter of the microbeads was calculated using ImageJ software.

Synthesis of PDMAPS by FRP

DMAPS (10 g, 35.8 mmol) and APS (50 mg, 0.21 mmol) were dissolved in deionized water (25 mL) in a three-neck round bottom flask equipped with a condenser. The polymerization was conducted at 85 °C for 2 h. After cooling down to room temperature, the as-synthesized polymers were precipitated from methanol and dried in vacuum oven for 12 h, yielding white fibrous **PDMAPS**.

UCST behavior of PDMAPS

An aqueous mixture of **PDMAPS** (10 mg) in water (10 mL) at 1 mg mL^{-1} was heated in a water bath at around 50 °C, forming an aqueous translucent mixture. Upon cooling to room temperature, the resulting mixture was analyzed by UV/vis spectroscopy to measure percentage transmittance at λ = 600 nm upon heating at a rate of 1 °C min^{-1} to 70 °C.

Fabrication of millimeter-sized beads (m-beads)

An aqueous transparent solution of ALG (200 mg) dissolved in water (10 mL) was mixed with the various amounts of **PDMAPS** of 0, 67, 670, and 2000 mg to form a series of m-beads with different amounts of ALG as 100%, 75%, 23% and 9%, referred as m-bead-100ALG, m-bead-75ALG, m-bead-23ALG, and m-bead-9ALG, respectively. The resulting mixtures were then heated in a water bath set at 50 °C. The formed aqueous translucent mixtures were added dropwise into a bath of 0.1 M aqueous $CaCl_2$ solution (50 mL) without stirring. After 10 min of stability period, the beads were collected and dried in air.

 © 2026 The Author(s). Published by the Royal Society of Chemistry

Open Access Article. Published on 19 January 2026. Downloaded on 3/14/2026 7:06:49 AM.
This article is licensed under a Creative Commons Attribution-NonCommercial 3.0 Unported Licence.

Encapsulation of fluorescein to fabricate fluorescent beads (FL-beads)

A similar procedure for fabrication of m-beads was adopted, with the exception of addition of fluorescein (40 mg) to aqueous translucent mixtures, resulting in the formation of a series of FL-beads.

UV/vis spectroscopy was used to determine the encapsulation efficiency (EE%) and loading content (LC%) of fluorescein. After the formation of FL-beads, aliquots of aqueous $CaCl_2$ solution (4 mL) were mixed with ethanol (16 mL). The resulting mixture solutions were passed through a disk-type PTFE filter (0.25 μm pore size) and their UV/vis spectra were recorded. The EE% and LC% were determined by the following equations:

$$\mathrm{EE\%} = \frac{\text{Weight of fluorescein encapsulated in m-beads}}{\text{Weight of feeding fluorescein}} \times 100\% \quad (1)$$

$$\mathrm{LC\%} = \frac{\text{Weight of fluorescein encapsulated in m-beads}}{\text{Weight of m-beads} + \text{encapsulated fluorescein}} \times 100\% \quad (2)$$

Release of fluorescein from FL-beads

After the removal of $CaCl_2$ solution from the bath, the fabricated FL-beads were mixed with fresh water (50 mL) at pH = 7.4. Aliquots of the aqueous solutions (4 mL) were taken for given time intervals and mixed with ethanol (16 mL, thus, water/ethanol = 1/4 v/v). Their UV-vis spectra were recorded for given time periods. Equal volume of fresh solution (4 mL) was added to keep the same volume of outer buffer solution.

For quantitative analysis, fluorescein (40 mg) was dissolved in water (50 mL) at pH = 7.4, to mimic aqueous fluorescein solution achieving 100% release. An aliquot (4 mL) was mixed with ethanol (16 mL) and its UV-vis spectrum was recorded. This was identified as the maximum quantity of fluorescein to be encapsulated and released. The absorbance value is used as the denominator to quantify the % release of fluorescein at different times.

Encapsulation of GFA to fabricate GFA-beads

A similar procedure for the encapsulation of fluorescein was applied, using GFA (40 mg) and 75% ALG composition. The EE% and LC% of GFA in the GFA-beads were determined using UV/vis spectroscopy, as described earlier.

Release of GFA from GFA-beads

The fabricated GFA-beads were mixed with fresh water (50 mL) at pH = 7.4 and aliquots of the aqueous solutions (4 mL) were taken for given time intervals and combined with ethanol (16 mL, thus, water/ethanol = 1/4 v/v). Their UV-vis spectra were recorded for the given time periods. An equal volume of fresh solution (4 mL) was added to keep the same volume of outer buffer solution.

For quantitative analysis, a series of aqueous solution of GFA at various concentrations ranging at 0.2–4 × 10^{-5} M were prepared. Their UV/vis spectra were recorded to construct a correlation curve of absorbance over concentration of GFA.

Results and discussion

The synthesis of **PDMAPS** was carried out in water *via* a free radical polymerization (FRP) for **DMAPS** monomer, initiated with APS, a water-soluble sulfate initiator (Fig. 1a). Upon complete monomer conversion, the purified **PDMAPS** was characterized by ^{1}H NMR spectroscopy for structural analysis (Fig. 1b). Since the formed **PDMAPS** had limited solubility in water, our ^{1}H NMR analysis was conduced in D_2O with the presence of NaCl salt, according to literature.[39] The characteristic peaks at 4.54 ppm (b) corresponding to methylene protons adjacent to ester group, 3.24 ppm (d) corresponding to methyl protons on the nitrogen, and 1.1–1.5 ppm (a) corresponding to methyl protons confirm the synthesis of **PDMAPS**. In a separate experiment, ^{1}H-NMR analysis was conducted at elevated temperatures for better resolution (see Fig. S1 for detailed analysis).

Both TGA and DSC were used to analyze the thermal properties of **PDMAPS**. The TGA diagram in Fig. 2a shows an initial

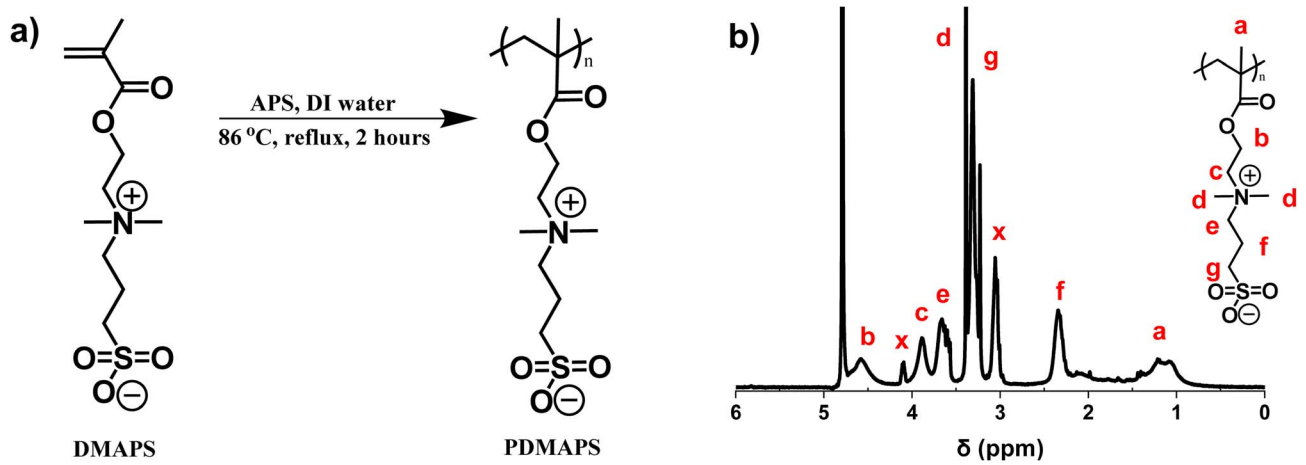

Fig. 1 Synthesis of **PDMAPS** by FRP of **DMAPS**, initiated with APS in water (a); ^{1}H-NMR spectrum in D_2O containing 0.5 M NaCl at 25 °C (b). Conditions for FRP: **DMAPS**/water = 0.4/1 (*e.g.*, 40 wt% **DMAPS** over water); 0.5 wt% of APS over **DMAPS**.

Open Access Article. Published on 19 January 2026. Downloaded on 3/14/2026 7:06:49 AM.
This article is licensed under a Creative Commons Attribution-NonCommercial 3.0 Unported Licence.

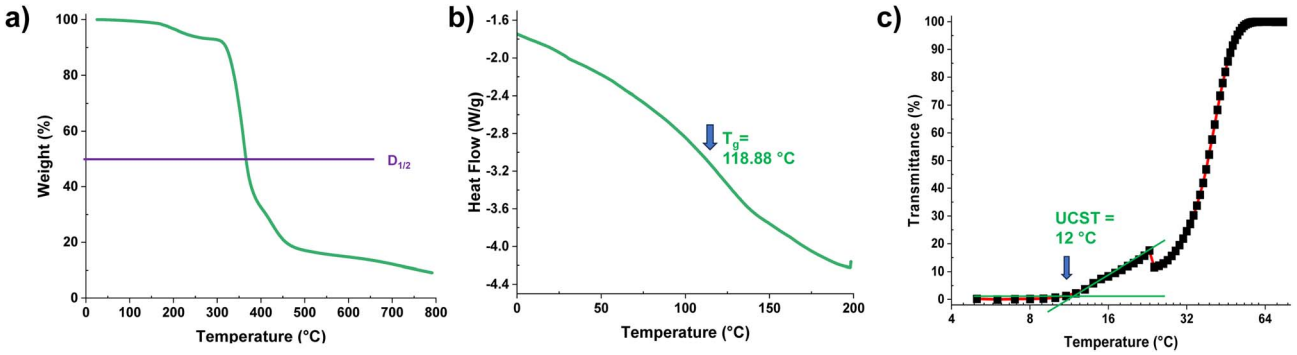

Fig. 2 TGA (a) and DSC (b) thermograms of **PDMAPS**; and % transmittance at $\lambda = 600$ nm over temperature on its aqueous solution at 1 mg mL^{-1} (c).

weight loss (<10%) at 180–290 °C, which could be attributed to either volatile species or oligomeric **PDMAPS**. The majority of the weight loss occurred between 290 and 430 °C, likely due to the decomposition of the organic material. There was also 10% residue weight. The $D_{1/2}$ defined as the temperature where the weight remains half was determined to be at 365 °C. The DSC diagram in Fig. 2b shows a single transition at 119 °C of the formed **PDMAPS**, which is in good agreement with the literature value for a bulk homo **PDMAPS**.[40]

UV/vis spectroscopy was examined to characterize the thermoresponsive property, particularly UCST of **PDMAPS**. The % transmittance at $\lambda = 600$ nm was recorded in the range of 5–75 °C on its aqueous solution at 1 mg mL^{-1}. As seen in Fig. 2c, a clear transition of % transmittance was detected. From the two linear progressions, the UCST of **PDMAPS** was determined to be 12 °C, which is in the range of values for **PDMAPS** prepared by controlled polymerization techniques reported in the literature.[41–43]

Next, we investigated the ability of **PDMAPS** to form beads. Our experiments revealed that the addition of aqueous **PDMAPS** solution into a gelling bath did not produce structurally stable beads. As such, we opted to mix **PDMAPS** with another material that could produce stable networks. Alginate (ALG) is a negatively charged natural polysaccharide containing β-(1,4)-D-mannuronic acid and α-(1,4)-L-guluronic acid monomers. It is biocompatible, environmentally friendly, biodegradable and economically favorable with unique physical and chemical properties.[44–46] Moreover, ALG can form structurally stable hydrogels in the presence of multivalent ions, typically calcium

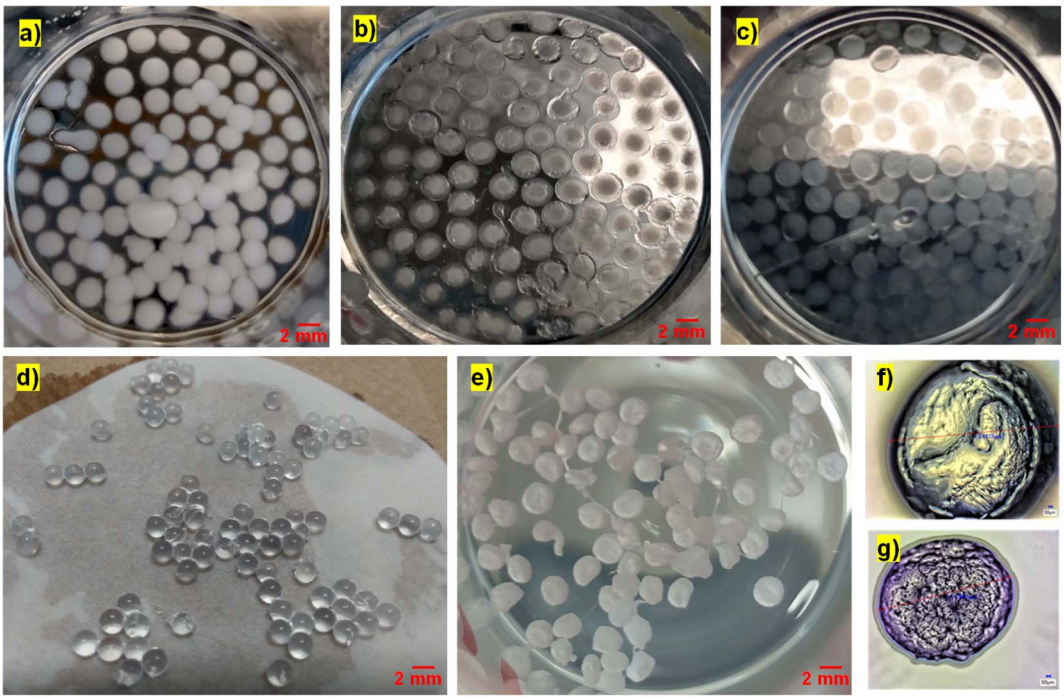

Fig. 3 Digital images illustrating the progressive formation of m-bead-9ALG over time at 0 (a), 5 (b), and 20 min (c) as well as digital images in wet (d) and dried state (e) and optical microscopy images in wet (f) and dried (g) state of m-bead-9ALG.

 © 2026 The Author(s). Published by the Royal Society of Chemistry

Open Access Article. Published on 19 January 2026. Downloaded on 3/14/2026 7:06:49 AM.
This article is licensed under a Creative Commons Attribution-NonCommercial 3.0 Unported Licence.

ion (Ca^{2+}), through supramolecular interactions of pendant carboxylic acid groups with Ca^{2+} ions.[47–51]

In our experiments, ALG was mixed with different amounts of **PDMAPS** and the resulting aqueous mixtures were added dropwise into a bath of aqueous solution containing Ca^{2+} ions. The fabricated m-beads were crosslinked through the supramolecular interactions of pendant carboxylic acids in ALG chains with Ca^{2+} ions. For m-bead-9ALG, containing 9% ALG as an example, the digital images shown in Fig. 3a–c illustrate the progress to form m-beads in aqueous solution over time (up to 20 min). The formed beads appeared to be transparent and spherical in wet state (Fig. 3d), while translucent and spherical in dried state (Fig. 3e). To get an insight into the fabrication of m-beads, the amount of ALG was increased to 23% and 75%, leading to an increase in not only physical crosslink density, but also the hydrophilicity of m-beads. All fabricated m-beads were structurally stable. Gravimetry analysis with their weights in wet and dried states was used to determine the water retention and swelling ratio. As presented in Table 1, m-beads with less than 25% ALG (*e.g.*, m-bead-9ALG and 25ALG) had water retention of 0.5–0.6 and swelling ratio of 2.2–2.4, while m-bead-75ALG had water retention of 0.99 and swelling ratio of 116. These results suggest that m-beads with higher ALG content exhibit greater water retention and swelling capacity than those with lower ALG content. This behavior is likely due to the dominant influence of hydrophilicity over supramolecular crosslink density in governing the water retention and swelling properties of the m-beads. Furthermore, the m-bead-9ALG was analyzed by optical microscopy and the images in Fig. 3f and g shows winkles and domains inside m-beads in both wet and dried states, with the average diameter estimated to be 1.9–2.5 mm for wet m-beads and 1.0–1.7 mm for dried m-beads.

Table 1 Solution properties of m-beads of PDMAPS prepared with various amounts of ALG

Beads	Weight (mg) Wet	Dried	Water retention[a]	Swelling[b]
m-bead-75ALG	23.2	0.2	0.99	116.0
m-bead-25ALG	7.8	3.6	0.54	2.2
m-bead-9ALG	7.8	3.2	0.59	2.4

[a] Weight ratio of (wet − dried)/wet. [b] Weight ratio of wet/dried.

The **PDMAPS** synthesized *via* FRP was not fully soluble in water but instead formed nanoaggregates with an average diameter of approximately 300 nm at temperatures below its UCST. Although **PDMAPS** has been reported to be miscible with ALG for the formation of composite hydrogels or interpenetrating polymer networks, in this study, aqueous mixtures comprising ALG chains and **PDMAPS** nanoaggregates were solidified and ionically crosslinked in a calcium chloride bath to yield m-beads. This observation suggests that **PDMAPS** and ALG were only partially miscible at the nanoaggregate interfaces, resulting in a degree of phase separation within the bead matrix. Additional morphological characterization will be required to provide a more comprehensive understanding of the internal structure and phase behavior of the composite m-beads.

The fabricated m-beads consisted of both thermoresponsive UCST **PDMAPS** and water-soluble ALG at various weight ratios. The feasibility of these composite beads for encapsulation and controlled release of agricultural chemicals was subsequently evaluated. Fluorescein, a water-soluble fluorescent dye, was selected as a model compound for our initial investigation. Using a similar procedure for fabrication, fluorescein was incorporated in the m-beads to yield a series of red-colored m-beads (FL-beads) with various amounts of ALG (9, 23, 75 and

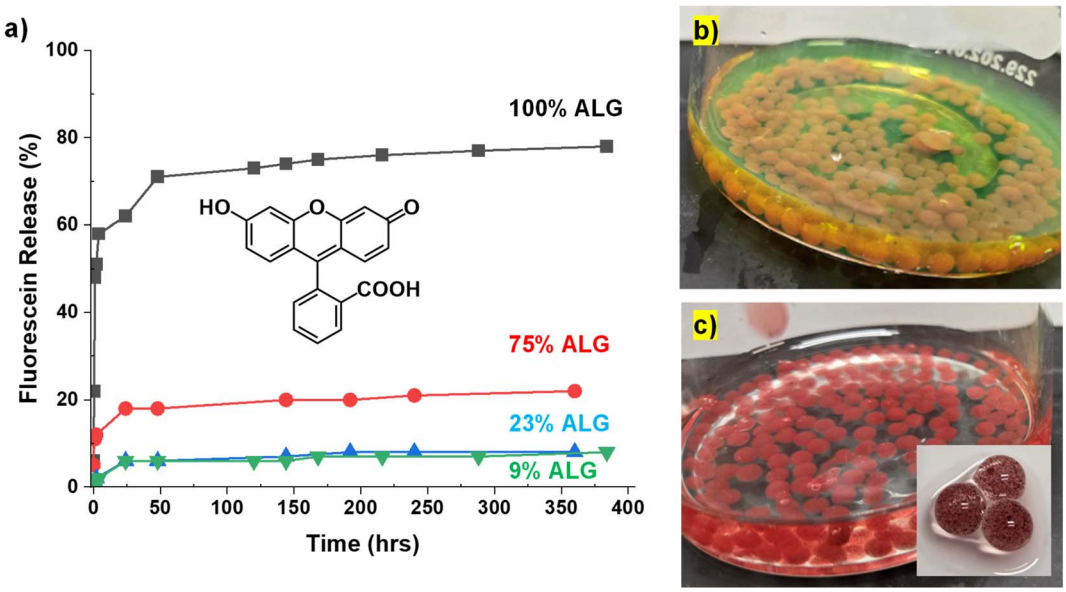

Fig. 4 % release of fluorescein of FL-beads prepared with various amounts of ALG at 25 °C (a) and digital images of FL-beads with 100% ALG (b) and 9% ALG (c and inset).

Open Access Article. Published on 19 January 2026. Downloaded on 3/14/2026 7:06:49 AM.
This article is licensed under a Creative Commons Attribution-NonCommercial 3.0 Unported Licence.

100 wt%). To test the encapsulation efficiency of fluorescein in FL-beads, UV/vis spectra were recorded for aqueous $CaCl_2$ gelling bath after the fabrication of FL-beads. No significant absorption of fluorescein was observed in the UV spectra, suggesting ≈100% encapsulation efficiency for all four FL-beads (Fig. S2). The loading level was determined to be 17% for m-bead-100ALG, 13% for m-bead-75ALG, 4% for m-bead-23ALG, and 2% for m-bead-9ALG, respectively. This result suggests that loading level decreased with an increasing amount of ALG in FL-beads.

Next, the controlled release of fluorescein from FL-beads was evaluated using UV/vis spectroscopy at room temperature. The UV/vis spectra of the surrounding aqueous medium was measured at the predetermined incubation intervals (Fig. S3). The absorbance at $\lambda = 480$ nm, along with the absorbance of fluorescein whose amount is equivalent to that encapsulated in each of FL-beads, were used to determine % release of fluorescein. Fig. 4a shows the results. For all FL-beads, the percentage release rapidly increased within 50 min, followed by a gradual rise over extended incubation. Notably, the release percentage increased progressively with the alginate content of the beads, following the trend 9 wt% < 25 wt% < 75 wt% < 100 wt%. This finding indicates that the release rate of fluorescein is positively correlated with the alginate concentration in the FL-beads, likely due to the higher hydrophilicity and increased matrix porosity imparted by alginate, which facilitate greater diffusion of the encapsulated compound into the surrounding medium. To further elucidate the release mechanism, the distribution and morphology of fluorescein within the FL-beads were examined. As shown in Fig. 4b, the digital image of the FL-beads composed of 100 wt% ALG in the hydrated state reveals a uniform distribution of fluorescein

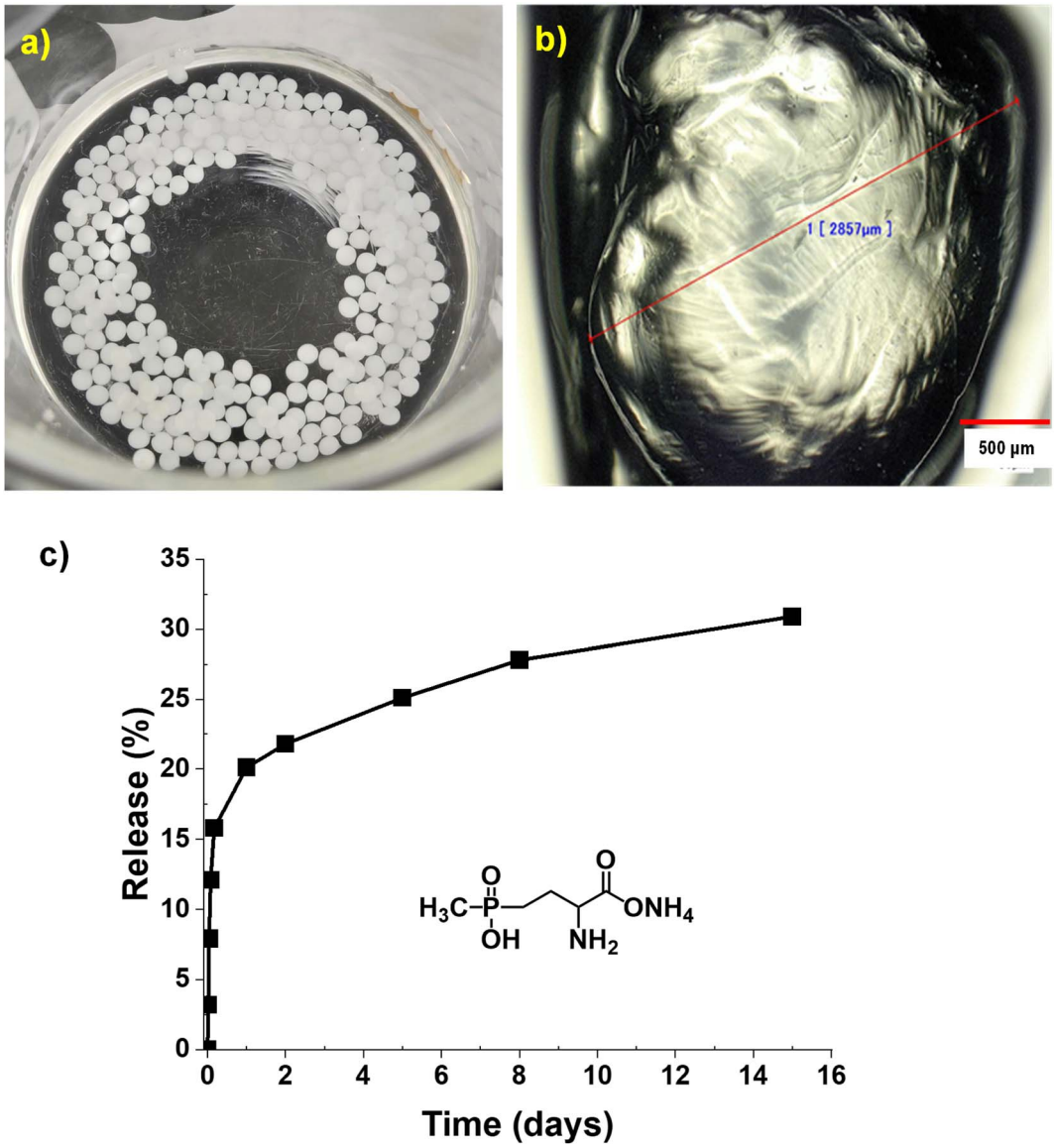

Fig. 5 Digital image (a) and optical microscopy image (b) of GFA-beads in wet state; release profile of GFA from GFA-bead (75% ALG) at 25 °C using UV/vis spectroscopy (c).

 © 2026 The Author(s). Published by the Royal Society of Chemistry

Open Access Article. Published on 19 January 2026. Downloaded on 3/14/2026 7:06:49 AM.
This article is licensed under a Creative Commons Attribution-NonCommercial 3.0 Unported Licence.

molecules, consistent with a diffusion-controlled release process. In contrast, the images of the FL-beads containing 9 wt% ALG (Fig. 4c and S4) show apparent segregation of fluorescein, likely localized within ALG-rich regions. This heterogeneous distribution suggests that the presence of **PDMAPS** nanoaggregates, with an average diameter of approximately 300 nm, may act as physical barriers to molecular diffusion, thereby retarding the release of fluorescein from beads with lower ALG content.

In a separate experiment, the release of fluorescein was conducted at 45 °C to get an insight into the effect of temperature with FL-beads/9% and 75% ALG. Fig. S5 compares their UV spectra taken after 4 h. For 9% FL-beads, % release was 27% at 45 °C, which is higher than 2% at 25 °C. For 75% FL-beads, it was as high as 45% at 45 °C than the 15% observed at 25 °C. These results suggest that the % release of fluorescein was enhanced at higher temperatures.

Given the results with the fluorescein dye, we studied the controlled release of GFA, a herbicide that has been proven to be effective against specific plant diseases and pests, making it essential asset in agricultural management.[52–54] A similar procedure was used to fabricate GFA-loaded m-beads containing 75% ALG (GFA-beads). The beads in wet state appeared to be opaque (see digital image in Fig. 5a). They had a diameter of 2.8–3.6 mm by optical microscope image (Fig. 5b), which is larger by approximately 1 mm, compared with bare m-beads. The reason was not clear but could be due to interactions between polymers and GFA. Our UV/vis spectroscopic experiment on aqueous Ca^{2+} solution in the bath reveals no significant absorption of GFA, indicating the efficiency to be ~100% (Fig. S6). The loading level of GFA was determined to be 13%.

For the release studies of GFA from GFA-beads, a correlation curve of absorbance at $\lambda = 314$ nm over the concentration of GFA in water was constructed (Fig. S7) and used for determining % GFA release. Fig. S8 shows the UV/vis spectra of aqueous medium recorded over the incubation intervals. As seen in Fig. 5c, GFA was released rapidly to 25% at initial 4 h and gradually increased to 30% over time up to 15 days, indicating the delayed release of GFA at 25 °C. One of the primary objectives of this work was to encapsulate the agricultural chemical to extend its residual life of the pesticide, thereby maintaining pesticidal efficacy over an extended period. Although the present data demonstrate controlled release within 15 days, the design of the m-beads is intended to enable sustained release of GFA well beyond this timeframe. Longer-term studies are currently planned to evaluate the extended-release behavior and persistence of GFA under simulated field conditions.

Conclusion

We fabricated thermoresponsive m-beads consisting of UCST polysulfobetaine and biodegradable ALG crosslinked through supramolecular ionic interactions. **PDMAPS** synthesized by solution FRP exhibited UCST transition at 12 °C, confirmed by UV/vis spectroscopy. The dropwise addition of aqueous mixture of **PDMAPS** with ALG into the bath of Ca^{2+} ion solutions resulted in the fabrication of structurally-stable m-beads. The encapsulation efficiency of both fluorescein and GFA in m-beads was as high as >98%. Their release rate increased with an increasing amount of ALG as well as at temperatures above UCST of **PDMAPS**, suggesting that the beads have promising release profile upon the change in daily temperature. These findings highlight the potential of **PDMAPS**/ALG-based microbeads as promising carriers for agricultural chemicals, paving the way for environmentally friendly, responsive delivery systems in precision agriculture.

Conflicts of interest

The authors declare no competing financial interest.

Data availability

The data collected throughout the course of the study are presented and detailed within the main sections of the manuscript and the supplementary information (SI). Supplementary information is available. See DOI: https://doi.org/10.1039/d5ra08674d.

Acknowledgements

This work was mainly supported by the National Research Council (NRC) through New Beginnings Initiative Ideation Fund as well as the Natural Science and Engineering Research Council (NSERC) in Canada through Discovery Grant. JKO was entitled Tier II CRC in Nanobioscience (2011–2021).

References

1 D. K. Ray, N. D. Mueller, P. C. West and J. A. Foley, *PLoS One*, 2013, **8**, e66428.
2 C. Zhao, B. Liu, S. Piao, X. Wang, D. B. Lobell, Y. Huang, M. Huang, Y. Yao, S. Bassu and P. Ciais, *Proc. Natl. Acad. Sci. U. S. A.*, 2017, **114**, 9326.
3 J. F. Andrade and E. H. Satorre, *Field Crops Res.*, 2015, **177**, 137.
4 R. Thakur and S. Sharma, Impact of pesticides used in agriculture: their benefits and hazards, *AIP Conf. Proc.*, 2024, **2986**, 030163.
5 Z. Li, *Rev. Environ. Contam. Toxicol.*, 2023, **261**, 14.
6 A. Sarker, D. Kim and W.-T. Jeong, *Sustainability*, 2024, **16**, 10741.
7 A. Zanino, F. Pizzetti, M. Masi and F. Rossi, *Eur. Polym. J.*, 2024, **203**, 112665.
8 A. Wijerathna, M. Evenden, P. Reid, B. Tidemann and H. Cárcamo, *J. Econ. Entomol.*, 2021, **114**, 1597–1606.
9 R. Tao, C. You, Q. Qu, X. Zhang, Y. Deng, W. Ma and C. Huang, *Environ. Sci.: Nano*, 2023, **10**, 351.
10 P. Fincheira, N. Hoffmann, G. Tortella, A. Ruiz, P. Cornejo, M. C. Diez, A. B. Seabra, A. Benavides-Mendoza and O. Rubilar, *Nanomaterials*, 2023, **13**, 1978.
11 J. L. de Oliveira, E. V. R. Campos, M. Bakshi, P. Abhilash and L. F. Fraceto, *Biotechnol. Adv.*, 2014, **32**, 1550.

Open Access Article. Published on 19 January 2026. Downloaded on 3/14/2026 7:06:49 AM.
This article is licensed under a Creative Commons Attribution-NonCommercial 3.0 Unported Licence.

12 M. A. C. Stuart, W. T. Huck, J. Genzer, M. Müller, C. Ober, M. Stamm, G. B. Sukhorukov, I. Szleifer, V. V. Tsukruk and M. Urban, *Nat. Mater.*, 2010, **9**, 101.
13 L. Chen, W. Zhang, H. Du, X. Ding, L. Li, H. Chen, F. Gao, B. Cui, J. Gao and H. Cui, *Chem. Eng. J.*, 2024, **483**, 149407.
14 V. Dhananjayan, S. Jayakumar and B. Ravichandran, in *Controlled Release of Pesticides for Sustainable Agriculture*, Springer, 2019, p. 1.
15 W.-H. Leong, S.-Y. Teh, M. M. Hossain, T. Nadarajaw, Z. Zabidi-Hussin, S.-Y. Chin, K.-S. Lai and S.-H. E. Lim, *J. Environ. Manage.*, 2020, **260**, 109987.
16 C. Bass and C. Jones, *Curr. Opin. Insect Sci.*, 2018, **27**, iv.
17 S. Mura, J. Nicolas and P. Couvreur, *Nat. Mater.*, 2013, **12**, 991.
18 C. J. F. Rijcken, O. Soga, W. E. Hennink and C. F. van Nostrum, *J. Controlled Release*, 2007, **120**, 131.
19 Q. Zhang, N. R. Ko and J. K. Oh, *Chem. Commun.*, 2012, **48**, 7542.
20 A. W. Jackson and D. A. Fulton, *Polym. Chem.*, 2013, **4**, 31.
21 Y. Wang, H. Xu and X. Zhang, *Adv. Mater.*, 2009, **21**, 2849.
22 K. Loomis, K. McNeeley and R. V. Bellamkonda, *Soft Matter*, 2011, **7**, 839.
23 A. P. Blum, J. K. Kammeyer, A. M. Rush, C. E. Callmann, M. E. Hahn and N. C. Gianneschi, *J. Am. Chem. Soc.*, 2015, **137**, 2140.
24 M. A. C. Stuart, W. T. S. Huck, J. Genzer, M. Muller, C. Ober, M. Stamm, G. B. Sukhorukov, I. Szleifer, V. V. Tsukruk, M. Urban, F. Winnik, S. Zauscher, I. Luzinov and S. Minko, *Nat. Mater.*, 2010, **9**, 101.
25 Y. Wang, X. Yu, S. Ma, S. Cao, X. Yuan, W. Zhu and H. Wang, *Green Chem.*, 2024, **26**, 42.
26 D. Zheng, B. Bai, H. Zhao, X. Xu, N. Hu and H. Wang, *Colloids Surf., B*, 2021, **207**, 112004.
27 M. Shen, S. Liu, C. Jiang, T. Zhang and W. Chen, *Eco-Environ. Health*, 2023, **2**, 161.
28 M. Zhao, P. Li, H. Zhou, L. Hao, H. Chen and X. Zhou, *Chem. Eng. J.*, 2022, **435**, 134861.
29 J.-D. Lavertu, K. K. Bawa, S. Hrapovic, D. Fu, J. K. Oh and U. D. Hemraz, *RSC Adv.*, 2024, **14**, 20105.
30 Y. Shen, C. An, J. Jiang, B. Huang, N. Li, C. Sun, C. Wang, S. Zhan, X. Li and F. Gao, *ACS Nano*, 2022, **16**, 20622.
31 M. C. Camara, E. V. R. Campos, R. A. Monteiro, A. do Espirito Santo Pereira, P. L. de Freitas Proença and L. F. Fraceto, *J. Nanobiotechnol.*, 2019, **17**, 100.
32 C. Ma, G. Li, W. Xu, H. Qu, H. Zhang, E. Bahojb Noruzi and H. Li, *J. Agric. Food Chem.*, 2024, **72**, 8906–8927.
33 J. Tang, X. Tong, Y. Chen, Y. Wu, Z. Zheng, A. B. Kayitmazer, A. Ahmad, N. Ramzan, J. Yang, Q. Huang and Y. Xu, *Nat. Commun.*, 2023, **14**, 6401.
34 M. Zhang, P. Yu, J. Xie and J. Li, *J. Mater. Chem. B*, 2022, **10**, 2338.
35 M. Boustta, P.-E. Colombo, S. Lenglet, S. Poujol and M. Vert, *J. Controlled Release*, 2014, **174**, 1.
36 Z. Wu, J. Fan, J. Hu, W. Xie, S. Sun, S. Hu, C. Li, Z. Wang and E. Ituen, *Int. J. Biol. Macromol.*, 2024, **268**, 131977.
37 V. Hildebrand, A. Laschewsky and D. Zehm, *J. Biomater. Sci., Polym. Ed.*, 2014, **25**, 1602.
38 Y. Lin, Y. Pang, Z. Li, M. Zhou, H. Lou and X. Qiu, *ACS Sustain. Chem. Eng.*, 2021, **9**, 15634.
39 H. Willcock, A. Lu, C. F. Hansell, E. Chapman, I. R. Collins and R. K. O'Reilly, *Polym. Chem.*, 2014, **5**, 1023.
40 K. Bauri, S. G. Roy, S. Arora, R. K. Dey, A. Goswami, G. Madras and P. De, *J. Therm. Anal. Calorim.*, 2012, **111**, 753.
41 Y. Zhu, J.-M. Noy, A. B. Lowe and P. J. Roth, *Polym. Chem.*, 2015, **6**, 5705.
42 Z. Li, H. Li, Z. Sun, B. Hao, T.-C. Lee, A. Feng, L. Zhang and S. H. Thang, *Polym. Chem.*, 2020, **11**, 3162.
43 Y. Nan, C. Zhao, G. Beaudoin and X. Zhu, *Macromol. Rapid Commun.*, 2023, **44**, 2300261.
44 M. Mollah, H. Zahid, Z. Mahal, M. Faruque and M. Khandaker, *Front. Mol. Biosci.*, 2021, **8**, 719972.
45 K. Y. Lee and D. J. Mooney, *Prog. Polym. Sci.*, 2012, **37**, 106.
46 I. P. S. Fernando, W. Lee, E. J. Han and G. Ahn, *Chem. Eng. J.*, 2020, **391**, 123823.
47 N. Pilipenko, O. H. Goncalves, E. Bona, I. P. Fernandes, J. A. Pinto, G. D. Sorita, F. V. Leimann and M. F. Barreiro, *Carbohydr. Polym.*, 2019, **223**, 115035.
48 X. Zhang, K. Wang, J. Hu, Y. Zhang, Y. Dai and F. Xia, *J. Mater. Chem. A*, 2020, **8**, 25390.
49 M. Bruchet and A. Melman, *Carbohydr. Polym.*, 2015, **131**, 57.
50 C. Lee, J. Shin, J. S. Lee, E. Byun, J. H. Ryu, S. H. Um, D.-I. Kim, H. Lee and S.-W. Cho, *Biomacromolecules*, 2013, **14**, 2004.
51 P. Xu, J. Song, Z. Dai, Y. Xu, D. Li and C. Wu, *Int. J. Biol. Macromol.*, 2021, **193**, 53.
52 G. Hoerlein, *Rev. Environ. Contam. Toxicol.*, 1994, **138**, 73.
53 A.-G. Calas, O. Richard, S. Même, J.-C. Beloeil, B.-T. Doan, T. Gefflaut, W. Même, W. E. Crusio, J. Pichon and C. Montécot, *Neurotoxicology*, 2008, **29**, 740.
54 S. O. Duke, Z. Pan, A. G. Chittiboyina, D. R. Swale and T. C. Sparks, *Pestic. Biochem. Physiol.*, 2023, **191**, 105340.

 © 2026 The Author(s). Published by the Royal Society of Chemistry